CrossMark

Brassica rapa var. *japonica* Leaf Extract Mediated Green Synthesis of Crystalline Silver Nanoparticles and Evaluation of Their Stability, Cytotoxicity and Antibacterial Activity

Mahmuda Akter[1] · **Md. Mostafizur Rahman**[1] · **A. K. M. Atique Ullah**[2] · **Md. Tajuddin Sikder**[3,4,5] · **Toshiyuki Hosokawa**[6] · **Takeshi Saito**[3] · **Masaaki Kurasaki**[1,4]

Abstract

Silver nanoparticles (AgNPs) were successfully synthesized from the reduction of Ag^+ using $AgNO_3$ solution as a precursor and *Brassica rapa* var. *japonica* leaf extract as a reducing and capping agent. This study was aimed at synthesis of AgNPs, exhibiting less toxicity with high antibacterial activity. The characterization of AgNPs was carried out using UV–Vis spectrometry, energy dispersive X-ray spectrometry, fourier transform infrared spectrometry, field emission scanning electron microscopy, X-ray diffraction, atomic absorption spectrometry, and transmission electron microscopy analyses. The analyses data revealed the successful synthesis of nano-crystalline Ag possessing more stability than commercial AgNPs. The cytotoxicity of Brassica AgNPs was compared with commercial AgNPs using in vitro PC12 cell model. Commercial AgNPs reduced cell viability to 23% (control 97%) and increased lactate dehydrogenase activity at a concentration of 3 ppm, whereas, Brassica AgNPs did not show any effects on both of the cytotoxicity parameters up to a concentration level of 10 ppm in PC12 cells. Moreover, Brassica AgNPs exhibited antibacterial activity in terms of zone of inhibition against *E. coli* (11.1 ± 0.5 mm) and *Enterobacter* sp. (15 ± 0.5 mm) which was higher than some previously reported green-synthesised AgNPs. Thus, this finding can be a matter of interest for the production and safe use of green-AgNPs in consumer products.

Keywords Silver nanoparticles · Green synthesis · PC12 cell · Cytotoxicity · *E. coli* · *Enterobacter* sp.

1 Introduction

Enormous uses of silver nanoparticles (AgNPs) in cosmetics have been increased in recent decades due to their unique physicochemical properties and antibacterial activities [1]. Recent researches have revealed that 12% of the total NPs used in cosmetics is AgNPs [2]. In particular, AgNPs have widely used in soaps, face creams, toothpastes, wet tissues, deodorants, lip products, face and body foams [1]. These huge applications of AgNPs could be threatening for human health, because the particles having size up to 1000 nm can across through skin and reach to inside of the cells [3]. Moreover, the absorption of NPs is enhanced in acne, eczema or wounds; subsequently the particles enter into the blood stream and induce complications [4]. It is also reported that, NPs (5–20 nm) can penetrate into the skin and interact with the immune system [5]. Besides, AgNPs could be penetrated through the human skin at a range of 0.2–2%, if barrier capacity in the skin was disrupted [6]. Several in vitro and in vivo studies revealed that AgNPs can induce

✉ Masaaki Kurasaki
kura@ees.hokudai.ac.jp

1   Graduate School of Environmental Science, Hokkaido University, Sapporo 060-0810, Japan

2   Chemistry Division, Atomic Energy Centre, Bangladesh Atomic Energy Commission, Dhaka 1000, Bangladesh

3   Faculty of Health Sciences, Hokkaido University, Sapporo, Japan

4   Faculty of Environmental Earth Science, Hokkaido University, Kita 10, Nishi 5, Kita-ku, Sapporo 060-0810, Japan

5   Department of Public Health and Informatics, Jahangirnagar University, Dhaka, Bangladesh

6   Research Division of Higher Education, Institute for the Advancement of Higher Education, Hokkaido University, Sapporo 060-0817, Japan

toxicity to organisms [7, 8]. The cytotoxic effects of AgNPs in A-549, NIH- 3T3, PC12 and HepG2 cell lines were reported in literature [9]. Prolonged effects of AgNPs were also warning for the possible adverse impacts on epigenetic dysregulation and gene expression reprogramming [10]. Hence, it is worthwhile to develop suitable method/s for the synthesis of AgNPs, which would be less toxic. Moreover, AgNPs having antibacterial activity could promote the safe use in dietary supplements, food packaging, cosmetics and anti-acne preparation. Consequently, it is important to establish a synthesis route of AgNPs having less toxicity with high antibacterial activity for the safe use of them in terms of human health concerns.

In recent years, numerous conventional methods are reported for AgNPs synthesis such as chemical reduction [11, 12], electrochemical [13], and sonochemical [14] processes. However, green synthesis method is being prominent as it is eco-friendly, cost effective and rapid with high substrate availability [15]. Green synthesis of AgNPs was firstly reported by Gardea-Torresdey et al. [16]. Chandran et al. [17] synthesized AgNPs using *Aloe vera* plant extract, and described that the presence of ammonia in the *Aloe vera* facilitated the bioreduction of Ag$^+$ ion for the formation of metallic AgNPs. The studies evaluated the use of plants and their tissues for AgNPs synthesis. *Aloe vera* leaf [18], *Musa paradisiaca* peels [19], *Cocos nucifera* coir [20], *Annona squamosa* peel [21], *Citrus aurantium* peel [22], and *Citrullus lanatus* rind [15] extracts mediated synthesis of AgNPs have been reported. The successful green synthesis can be a potential candidate to replace conventional chemical synthesis of NPs. Thus, scientists all over the world have been searching for the new substrates from the nature. However, to the best of our knowledge there is no report available on AgNPs synthesis using *Brassica rapa* var. *japonica* leaf extract. *Brassica rapa* var. *japonica* plant (locally known as Mizuna) belongs to the mustard family, and has long, broad, serrated and deeply cut finished leaves with thin trailing stems. It flavours as bright piquant with a slight earthiness, and contains vitamins A, C, and E with high glucosinolate compounds [23]. Moreover, *Brassica rapa* var. *japonica* grows almost round the year in Japan, China and Korea, and it is very popular in salad, soup and hot pot. Therefore, *Brassica rapa* var. *japonica* leaf extract can be a potential candidate as a source of reducing and capping agent for the green synthesis of AgNPs.

The aim of this study was to establish a method of synthesis of crystalline AgNPs, as crystalline materials are generally known as more stable than the amorphous phase, to ensure their stability in biological medium in order to show less toxicity along with enhanced antibacterial activity. The toxicity of AgNPs on cells was evaluated from the cell viability and LDH assay experiments from their exposure to PC12 cells, a well known model cell line in molecular biology to

assess cytotoxicity [24]. The antibacterial activity of AgNPs was assessed using *E. coli* and *Enterobacter* sp. *E. coli* is a coliform gram negative bacteria which is considered as the best biological indicator of drinking water and widely used in bacterial study [25–27]. It is abundant on the body surface of mammals and sometimes results acute infection [28]. *Enterobacter* sp. is a pathogenic bacteria cause nosocomial infection and can be replicated easily in contaminated fluid [29]. Finally, the cytotoxic effect of *Brassica rapa* var. *japonica* leaf extract mediated green synthesized AgNPs was compared with commercially available AgNPs and the antibacterial activity was compared with some of other reported green synthesized AgNPs.

2 Materials and Methods

2.1 Materials

Commercially available 10 nm sized AgNPs was purchased from Sigma Aldrich (St. Louis Missouri, USA). 0.1 M AgNO$_3$ was purchased from Wako Pure Chemical Industries (Osaka, Japan). *Brassica rapa* var. *japonica* plants were collected locally from Sapporo, Japan. PC12 cell line was obtained from the American type culture collection (USA and Canada). Dulbacos modified eagles medium (DMEM) was purchased from Sigma (St. Louis, MO, USA). Fetal bovine serum was purchased from Biosera (Kansas City, MO, USA). Trypan blue stain solution (4%) was purchased from Bio Rad (Hercules, CA, USA). Bacto trypton, bacto agar and yeast extract were purchased from Difco Laboratories (Detroit, MI, USA), and sodium chloride from Wako Pure Chemical Company (Osaka, Japan). All other reagents and chemicals used in this study were of analytical grade.

2.2 Preparation of *Brassica rapa* var. *japonica* Leaf Extract

Fresh and healthy leaves of *Brassica rapa* var. *japonica* were collected locally and then thoroughly washed with tap water followed by distilled water for several times to remove the visible dust. Then, the leaves were dried naturally for 10 days, and blended with a blender to make leaf powder. After that, 1 g of leaf powder was mixed with 50 mL of distilled water and boiled at 100 °C for 10 min. After cooling at room temperature (25 °C), the leaf broth was filtered through Whatman filter paper (Catalogue No. 5211-0900). The filtrates were then stored at 4 °C for further experiments.

2.3 Synthesis of AgNPs Using *Brassica rapa* var. *japonica* Leaf Extract

In this study, 10 mL of *Brassica rapa* var. *japonica* leaf extract was added with 100 mL of 1 mM AgNO$_3$ solution

drop wise at a rate of around one drop per second under constant stirring on a magnetic stirrer. The stirring was continued for 1 h and then kept undisturbed at room temperature (25 °C) for 24 h. The reduction of Ag^+ ions to Ag^0 was monitored by the change of colour from gray to reddish yellow. The broth was then centrifuged at 10,000 rpm for 10 min and the precipitates were washed with deionized water and centrifuged repeatedly to remove the impurities. The precipitates were dried at 60 °C for overnight, and stored in a desiccator for further analysis.

2.4 UV–Vis. Spectra Analysis

The formation of AgNPs from the reduction of Ag^+ ion was analyzed by monitoring the UV–Vis. spectra. Sample was diluted for 20 times with deionized water and spectra of Brassica AgNPs and commercial AgNPs suspension were recorded at wavelength of 200–700 nm using a UV–Vis. spectrophotometer (JASCO V-650, Japan). During the experiment, deionized water was used as blank to adjust the baseline of the UV–Vis. spectra. This experiment was repeated three times for the reproducibility.

2.5 Field Emission Scanning Electron Microscopy (FESEM) and Energy Dispersive X-Ray (EDX) Spectrometry Analyses of AgNPs

The surface morphology of AgNPs was monitored using FESEM (JEOL, model JSM 6500 F, Japan). The elemental composition was obtained from EDX spectrometer (JEOL, model JSM 6500 F, Japan). The operating condition of the instrument was 15 kV acceleration voltage and 12 µA emission current.

2.6 X-Ray Diffraction (XRD) Analysis of AgNPs

Crystalline phase was measured by XRD technique (Rigaku, MiniFlex, Japan). During XRD, sample was placed on XRD grid and spectra were recorded at 40 keV and 30 mA of voltage and current respectively with Cu Kα radiation.

2.7 Transmission Electron Microscopy (TEM) Analysis of AgNPs

The sizes of AgNPs were measured by TEM (JEOL, JEM 2010, Japan). A suspension of AgNPs with ethanol was prepared, and 1 µL of the suspension was placed on formver coated grid, allowed to dry at room temperature (25 °C) and then kept on a specimen holder in order to perform TEM analysis. The images were viewed at an accelerating voltage of 120 kV.

2.8 Fourier Transform Infrared (FT-IR) Analysis

FT-IR spectra of AgNPs and *Brassica rapa* var. *japonica* leaf powder were recorded to find the presence of functional groups that bound distinctively with the AgNPs surfaces. 1% (w/w) samples were mixed with KBr powder, and pressed into a sheer slice. FT-IR spectra of the samples were measured from 500 to 5000 cm^{-1} with a JASCO FT/IR-4100, Japan.

2.9 Assessment of Stability of AgNPs

The stability of AgNPs was assessed from the silver ion release test measured by atomic absorption spectrophotometer (AAS) (HITACHI, model U-135, Kyoto, Japan). Hollow cathode lamp with 7.5 mA lamp current, 328.1 nm wave length and 0.3 nm slit was used in the AAS. The purity of C_2H_2 gas was 99.99%. 1 ppm suspensions of both commercial and Brassica AgNPs were prepared with deionised water and kept at room temperature (25 °C) for 1 h and 24 h respectively. Suspensions were centrifuged at 3000 rpm for 5 min before taking the absorbance. To ensure the reproducibility of the results, silver ion release test was performed for three times.

2.10 Assessment of Cytotoxicity of AgNPs

2.10.1 Cell Viability Assay

PC12 cells were cultured in DMEM medium supplemented with 10% FBS in a humidified incubator at 37 °C with 5% CO_2 in 25 cm^2 culture flasks. Then, the AgNPs were added into the flasks, and incubated for 48 h. In every treatment, fresh medium was added prior to treatment. The cell viability of PC12 cells after the exposure of AgNPs was measured by trypan blue exclusion assay method [30]. After 48 h incubation with AgNPs exposure, cell viability was measured using Bio-Rad automated cell counter (Herculis CA, USA). Cell viability was expressed as percentage of the total cell counts against the stained cell counts. Each experiment was performed at least three times to make sure the reproducibility and statistical validity.

2.10.2 Lactate Dehydrogenase Activity (LDH) Assay

The LDH activity in the treatment medium after the exposure of AgNPs to PC 12 cells was measured using a nonradioactive cytotoxicity assay kit (Promega, state of Wisconsin, WI, USA) [31]. The cells were cultured in a medium and treated with 0, 1 and 3 ppm of AgNPs. After 48 h cultivation, 50 µL medium was taken into a 1.5 mL eppendorf tube, and then substrate mixture containing tetrazolium salts was added. After 30 min incubation at room temperature, stop

solution was added, and the total amount of formazan dye formed was determined by measuring absorbance at 490 nm using DU65 spectrophotometer (Beckman, CA, USA). LDH assay was also performed at least three times to ensure reproducibility and statistical validity.

2.11 Antibacterial Activity of Brassica AgNPs

The antibacterial activity of AgNPs was measured by disc diffusion method [32]. *E. coli* (JM-109 strain) and *Enterobacter* sp. were used as gram negative bacteria. Bacteria were cultured in Luria Broth (LB) medium (tryptone 1.5%, yeast extract 0.75%, sodium chloride 1.2%) at 37 °C with 60 rpm shaking in water bath. Fresh culture containing 6.6×10^6 bacteria measured by the optical density at 600 nm was used for the experiments [33]. To measure the inhibition zone, 50 μL of medium containing bacteria were poured into LB plate with 1% agar. For disc preparation, filter paper was punched, autoclaved and dried at 60 °C for overnight. Subsequently, the discs (5 mm sized) were soaked with 15 μL of AgNPs suspensions and placed on culture plate at 37 °C for 24 h.

2.12 Statistical Analyses

To ensure the reproducibility of the results, each of the experiments was repeated at least three times. Statistical analyses were conducted following unpaired student's *t* test. All data were presented as the mean ± standard error of mean (SEM). Significance level was calculated at $p < 0.05$, where difference between means were considered as statistically significant.

3 Results

3.1 Characterization of AgNPs

The formation of AgNPs through the reduction of Ag^+ was primarily monitored using UV–Vis. spectra analysis. It is reported that AgNPs exhibit UV–Vis. absorption maxima at wavelength range of 400–500 nm because of the surface plasma resonance [18]. In the present study, an absorption peak was observed at 450 nm after 1 h reaction as shown in Fig. 1, indicating the formation of metallic AgNPs [18]. In addition, in commercial AgNPs, a broad peak at 450 nm was also observed. Dispersion and aggregation of both *Brassica rapa* var. *japonica* mediated AgNPs (Brassica AgNPs) and commercial AgNPs (Com AgNPs) were examined using FESEM as shown in Fig. 2a, b, respectively. From the images, it was evidenced that both the Brassica and Com AgNPs were uniformly dispersed, referred a very few aggregation of particles. EDX analysis confirmed the
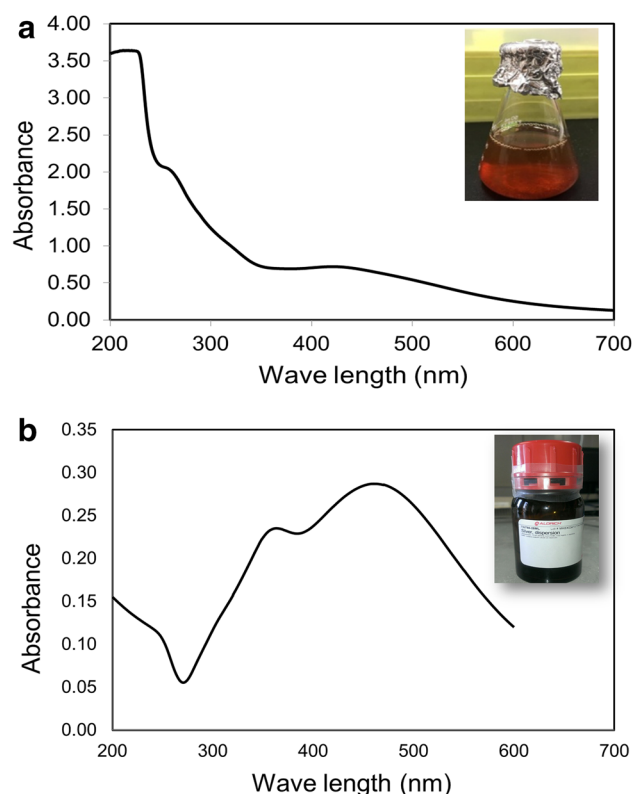

Fig. 1 UV-Vis. absorption spectra of AgNPs. Brassica AgNPs (**a**) and Com AgNPs (**b**) show absorption spectra at 450 nm in UV-Vis. spectrometer

presence of high percentage of elemental silver signalling strong peak as shown in Fig. 3. However, some weaker peaks were also found for oxygen and carbon in Brassica AgNPs. Crystallinity and solid phase microstructure of Brassica AgNPs was characterized by XRD (Fig. 4) at a scanning range of 35°–85° (2θ). Five distinct diffraction peaks were found at 38.04°, 44.24°, 64.4°, 77.24° and 81.48°, which were indexed as the planes 111, 200, 220, 311 and 222 respectively. The crystalline phase was found to be cubic and the value of lattice constant was measured using Nelson–Riley function [34]. The average lattice constant was found to be 4.0904 Å which agreed with reported value [35]. The crystallite size was calculated using Debye–Scherrer approximation [36, 37] and the value was found to be 15 nm. Moreover, from TEM analysis, size and surface morphologies was observed and it was revealed that both types of AgNPs were of spherical in shape (Fig. 5a, b). The sizes were ranged from 15 to 30 nm and 10 to 15 nm for Brassica and Com AgNPs, respectively. The size of Brassica Ag NPs measured from the TEM analysis agreed with the crystallite size calculated from the XRD patterns. Finally, FT-IR spectra showed the functional groups present in *Brassica rapa* var. *japonica* leaf biomass and Brassica AgNPs (Fig. 6a) and also Com AgNPs (Fig. 6b). The strong band at 1072.23 cm^{-1}

Fig. 2 FESEM (Field emission scanning electron micrograph) shows evenly dispersed **a** Brassica AgNPs and **b** Com Ag NPs
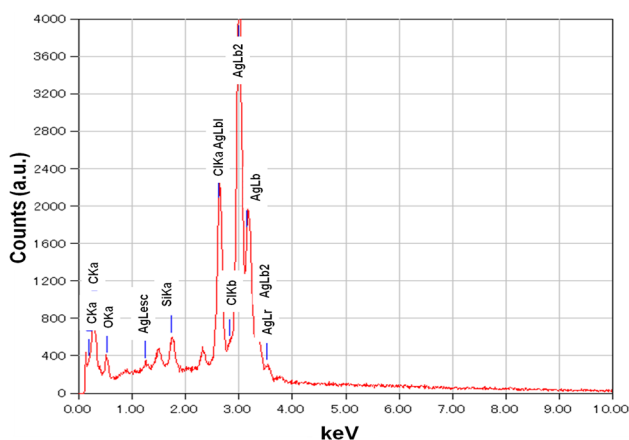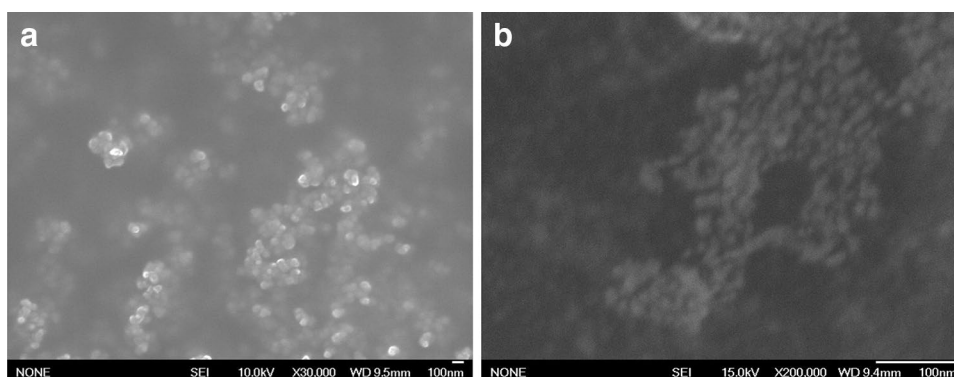
Fig. 3 EDX (Energy dispersive X-ray) of Brassica AgNPs shows strong metal peak for silver with some weaker peaks for carbon and oxygen
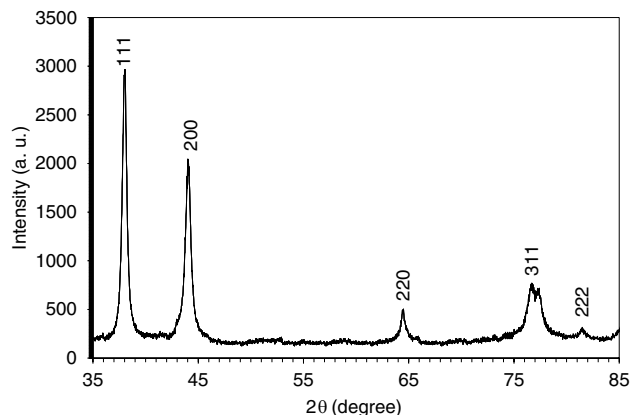
Fig. 4 XRD (X-ray diffraction) pattern of Brassica AgNPs demonstrating crystalline phase of nanosilver

corresponded to the C=O or C–O–C stretches, 1634.38 cm^{-1} referred to –C=C stretch. Signals of 1800 and 2361.41 cm^{-1} indicated –C=O and –C≡C groups, respectively. Broad peak at 3409.53 cm^{-1} and weak peak at 630 cm^{-1} corresponded to the presence of –NH and C–H groups, respectively [38].

3.2 Stability Assessment of AgNPs

One ppm of both Brassica AgNPs and Com AgNPs were taken and release of ion was measured after 1 and 24 h incubation under room temperature. Released ion from Brassica AgNPs was measured as 0.014 and 0.120 ppm after 1 and 24 h incubation respectively (Fig. 7) whereas, with the same incubation, released ion was measured as 0.628 and 0.937 ppm respectively for Com AgNPs (Fig. 7).

3.3 Cytotoxicity Analysis of AgNPs

3.3.1 Cell Viability Assay

To assess the relative cytotoxicity of Brassica and Com AgNPs, both types of NPs at different concentrations were exposed to PC12 cells. Then cell viability was measured by trypan blue exclusion method at 48 h-after incubation with/without NPs exposures. In case of Com AgNPs, the cell viability was decreased in a concentration dependent manner, whereas, for Brassica AgNPs the cell viability showed almost same for all treatment groups of 0, 1 and 3 ppm of Brassica AgNPs (Fig. 8). The cell viability study showed that up to 9 ppm of Brassica AgNPs have no cytotoxic effects on PC12 cells for 48 h of incubation (Fig. 9).

3.3.2 LDH Assay

To confirm whether Brassica AgNPs have no cytotoxicity, LDH activity in the culture medium of PC12 cells treated with Brassica and Com AgNPs were measured. A significant difference of LDH activity between the Com AgNPs-treated group (1 and 3 ppm) and control group was observed but no significant change was observed between control group and Brassica AgNPs-treated groups. However, a significant difference was found between Com AgNPs and Brassica AgNPs in both applied concentrations (Fig. 10). The LDH activity results corroborated with the cell viability assay results, however, both assays confirmed the Brassica AgNPs showed less cytotoxicity than the Com AgNPs in PC12 cells.
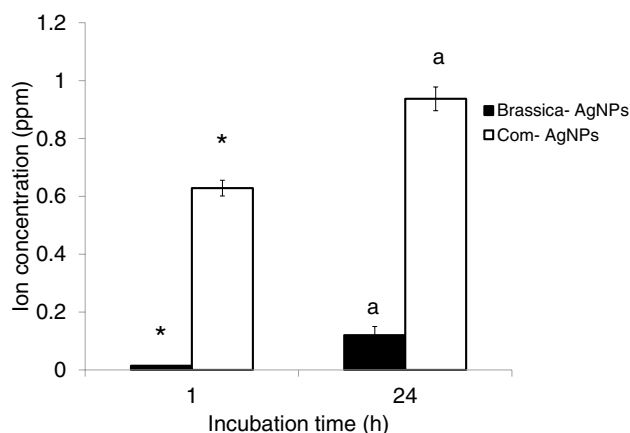
Fig. 5 TEM (Transmission electron micrograph) shows **a** spherical shaped Brassica AgNPs with the size range from 15 to 30 nm and **b** spherical shaped Com AgNPs with the size range from 10 to 15 nm
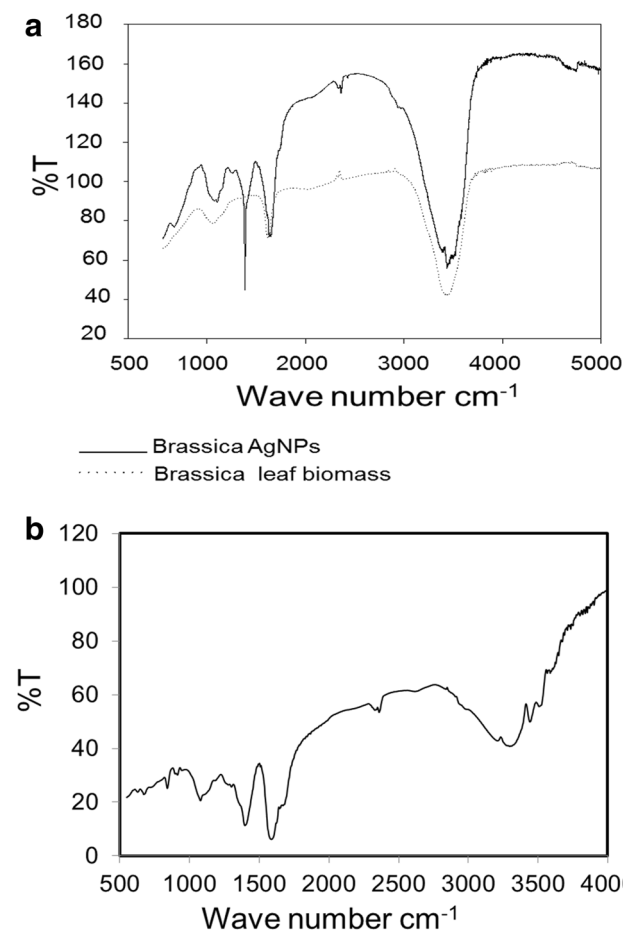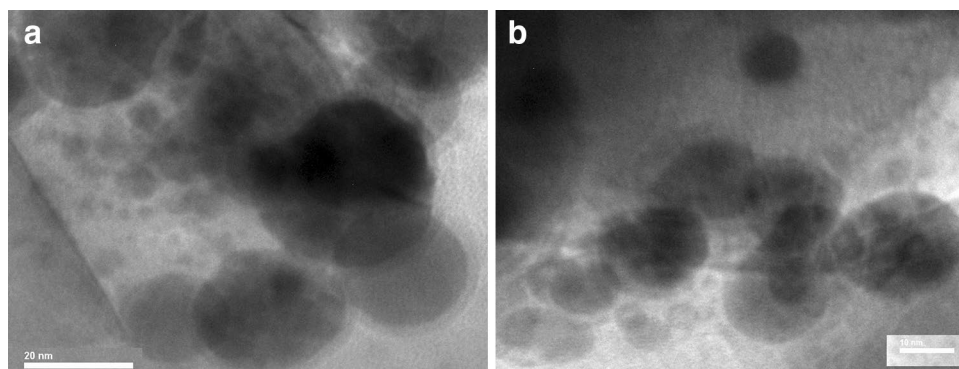
Fig. 6 FT-IR (Fourier Transmission Infrared Spectroscopy) absorption spectra of **a** Mizuna (*Brassica rapa*. var. *japonica*) leaf biomass (solid line) and (dashed line) Brassica AgNPs and **b** Com AgNPs

Fig. 7 Silver ion release from Brassica AgNPs and Com AgNPs after 1 and 24 h incubation. Error bars indicate mean ± SEM (n = 3). Asterisk * denotes significant change from Com AgNPs to Brassica AgNPs at 1 h incubation and "*a*" denotes significant change from Com AgNPs to Brassica AgNPs at 24 h incubation at $p < 0.05$

3.4 Antibacterial Activity Analysis

The antibacterial activity of Brassica AgNPs was assessed in terms of the zone of inhibition (ZOI) measurement against two gram negative bacteria, *E. coli* and *Enterobacter* sp. Amphicillin disc and blank disc were used as positive and negative controls, respectively. There was no effect on

bacterial growth was found for the negative control whereas, the positive control showed a clear ZOI. Using different concentrations (10, 100, 1000 and 2000 ppm) of Brassica AgNPs disc, a clear ZOI was detected for both of the *E. coli* (Fig. 11a) and *Enterobacter* sp. (Fig. 11b).

4 Discussion

The huge uses of AgNPs particularly, in cosmetics raise a grave concern for their toxicity [39, 40]. We have shown in our previous review study that AgNPs can induce toxicity in different cell lines [2]. Consequently, to ensure the safe applications of AgNPs in consumer products it was aimed to establish a suitable synthesis method for AgNPs having less toxicity and high antibacterial activity; moreover, it was desirable that this development would be environmentally friendly and cost effective. In this study, for the synthesis of novel green AgNPs, AgNO$_3$ solution was taken as a
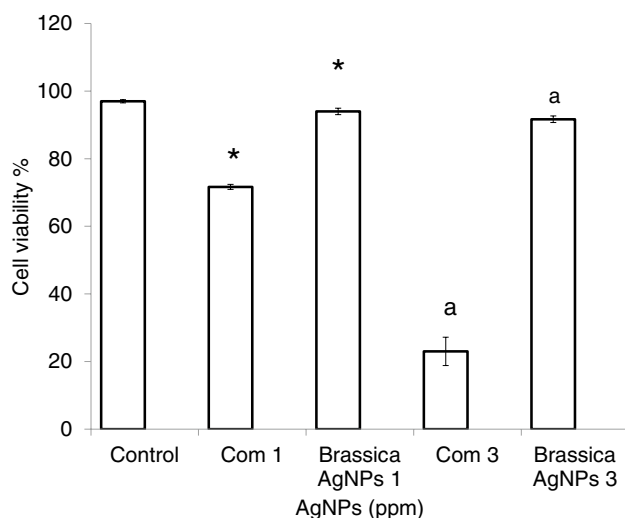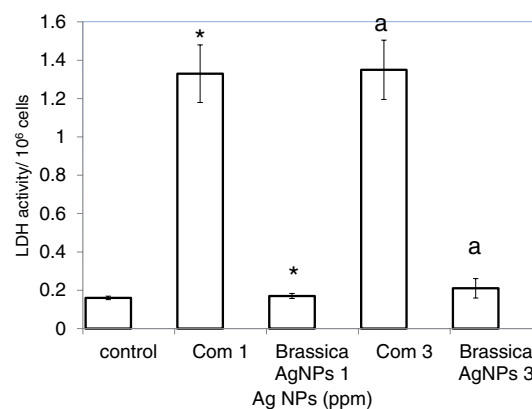
Fig. 8 Cell viability of PC12 cells measured by trypan blue staining method with/without treated by com AgNPs and Brassica AgNPs in different concentrations (1, 3 ppm) for 24 h of incubation. Control group contains cells with medium. Error bars indicate mean ± S.E.M (n = 3). Asterisk * denotes significant change from com AgNPs (1 ppm) to Brassica AgNPs (1 ppm) and "a" denotes significant change from com AgNPs (3 ppm) to bio AgNPs (3 ppm) at $p < 0.05$
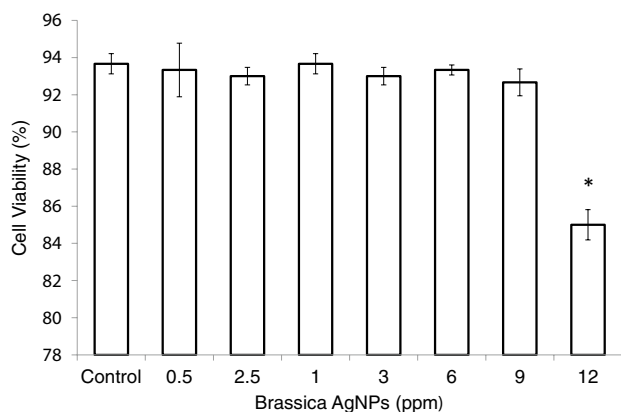
Fig. 9 Cell viability of PC12 cells measured by trypan blue staining method with treatment to Brassica AgNPs in different concentrations (0.5, 2.5, 1, 3, 6, 9, 12 ppm) for 48 h of incubation. Control group contains only cells with medium. Error bars indicate mean ± S.E.M (n = 3). Asterisk * denotes significant change from control group to Brassica AgNPs treated group at $p < 0.05$


Fig. 10 Lactate dehydrogenase (LDH) activity in the culture medium of PC12 cells after treatment with/without com AgNPs and Brassica AgNPs after 48 h of incubation. Error bars indicate mean ± S.E.M (n = 3). Asterisk * denotes significant change of LDH activity from com AgNPs (1 ppm) to Brassica AgNPs (1 ppm) "a" denotes significant change from com AgNPs (3 ppm) to Brassica AgNPs (3 ppm) at $p < 0.05$

precursor, and *Brassica rapa* var. *japonica* leaf extract was chosen as a source of reducing and capping agent.

A successful reduction of Ag^+ to $Ag°$ was visualized through the distinct change of colour from gray to reddish yellow due to AgNPs formation [41]. It is well established that this reddish yellow colour arises, due to the excitation of Surface Plasmon Resonance (SPR) vibration occur in the AgNPs [42]. Furthermore, from the UV–Vis. spectrometry, the formation of AgNPs in the Ag suspension was also evident. A strong peak was appeared at the wavelength of 450 nm indicating the presence of metallic nano silver, resulted from the reduction of Ag^+ [42, 43]. Moreover, in case of Com AgNPs, a broad peak was also obtained at 450 nm similar to Brassica AgNPs confirming the formation of Brassica Ag NPs.

The FESEM images depicted the presence of AgNPs with minimal agglomeration for both the Brassica AgNPs and Com AgNPs (Fig. 2a, b), which might be due to the presence of phytochemicals and sodium citrate that stabilized the particles, respectively [44]. EDX spectra of Brassica AgNPs revealed the elemental nature of AgNPs. Elemental silver showed a signature peak at 3 keV (Fig. 3). Several weaker peaks were also found corresponding to materials containing carbon and oxygen which might be originated from *Brassica rapa* var. *japonica* leaf extract. Crystalline formation of newly synthesized Brassica AgNPs was further confirmed by XRD analysis. Five distinct characteristic peaks were observed at $2\theta = 38.04°$, 44.24°, 64.4°, 77.24° and 81.48° corresponded to the planes 111, 200, 220, 311 and 222 respectively (Fig. 4), which were identified as face cantered cubic Ag in accordance with JCPDS card of Ag (JCPDS Card number 87-0597) [45]. The value of lattice constant was calculated as 4.0904 Å which was in good agreement with the earlier work [35].

The size and surface morphologies of both Brassica and Com AgNPs was assessed by TEM analysis. The TEM images showed that AgNPs were spherical in shape with smooth edges in both Brassica and Com AgNPs. The sizes of both Brassica and Com AgNPs were also measured as about 15–30 and 10–15 nm, respectively (Fig. 5a, b) which supported with the crystallite size calculated from

Fig. 11 Antibacterial activity of Brassica AgNPs to *E. coli* (JM-109) in terms of zone of inhibition (ZOI) at a concentration of **a** 10 ppm, **b** 100 ppm **c** 1000 ppm and **d** 2000 ppm. 1, 2, 3 denotes blank, Brassica AgNPs and amphicillin, respectively. Amphicillin represents positive control and blank represents negative control as well. Antibacterial activity was carried out three times for ensuring biological reproducibility

(10 ppm)   (100 ppm)
(1000 ppm)   (2000 ppm)
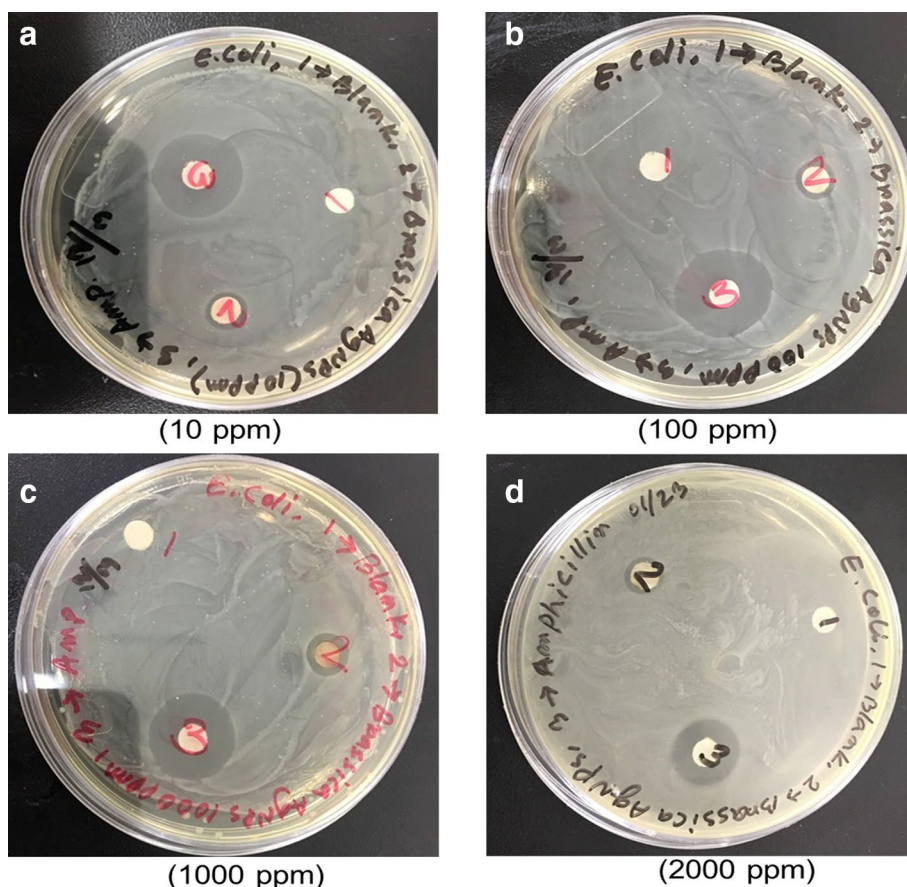
the XRD patterns of Brassica AgNPs. C=O and N–H stretching found in the FT-IR spectra might be due to the presence of amino acids in plant biomass. The functional groups such as –C≡C and C–H obtained due to the presence of anthracene. Functional groups C–O, –C–O–C and –C=C referred to heterocyclic compounds like alkaloid, flavones and anthracenes [42]. Similiar functional groups found in Brassica AgNPs and Brassica leaf biomass (Fig. 6a) might be suggested that, the amino acids (R-CH(NH$_2$)–COOH) containing lone pairs of electrons were acted as source of reducing agents that are capable of the reduction of Ag$^+$ for the formation of metallic AgNPs in ambient condition [46]. Moreover, alkaloid, flavones and anthracenes present in leaf extract were acted as a capping agent of AgNPs [42] that stabilizes the AgNPs, whereas, in Com AgNPs, no distinct peak was found in FT-IR (Fig. 6b), suggesting the absence of any functional groups in Com AgNPs.

From the stability assay performed by AAS analysis it was found that Brassica AgNPs showed more stability than Com AgNPs which agreed with the results of XRD, EDX and FT-IR analyses. This might be due to the crystalline nature of Brassica Ag NPs, confirmed from the XRD patterns and due to the presence of capping agent on Brassica AgNPs confirmed from the EDX and FT-IR analyses.

To evaluate the comparative cytotoxicity of Brassica and Com AgNPs, both types of NPs were exposed to PC12 cells, a widely used model cell line for toxicity assessment. It is reported that commercially synthesized AgNPs induce toxicity in different cell lines, e.g., HeLa, U937 [47], and human hepatoma cell line [48]. In our study, Com AgNPs showed a significant decrease of cell viability of PC12 cells in a concentration dependent manner, whereas, no significant change was observed for Brassica AgNPs in the same condition (Fig. 8). It was observed that the cell viability was decreased up to 77% with the exposure of 3 ppm of Com AgNPs, whereas cell viability of the cells exposed with 3 ppm of Brassica AgNPs showed almost the same as control. However, a significant decrease in cell viability was obtained for the exposure of Brassica AgNPs for 12 ppm (Fig. 9). It was reported that 7–20 nm sized Com AgNPs showed toxicity on A431 cell line where toxicity threshold was measured at 1.56 ppm [49]. However, 15–25 nm size of Brassica AgNPs significantly reduced cell viability at a concentration of 12 ppm on PC12 cells (Fig. 9). LDH activity measurements (Fig. 10) supported the same manner for Com AgNPs (showing toxicity) and Brassica AgNPs (showing no toxicity) compared as cell viability experiments. LDH activity determines cell membrane integrity [50], therefore, increased trend of LDH activity was a sign of more cell

damage in response to toxic effects. Recently, different biogenic materials have been used for AgNPs synthesis. In Table 1, we compared cytotoxic effect of Brassica AgNPs with various source mediated green synthesised AgNPs. AgNPs synthesized from *Albizia adianthifolia* [51], *S. grandiflora* leaf extract [46] and watermelon rind extract [15] induce toxicity in different cell line at a concentration of 10, 5 and 4 ppm respectively. Comparing to those green synthesized AgNPs, Brassica AgNPs showed less toxicity than other phytosynthesized AgNPs, but chitosan [52] and fungi [53] synthesized AgNPs appeared less toxic than any other phytosynthesized AgNPs. In addition, commercial AgNPs showed severe toxicity comparing green synthesised AgNPs [47].

The mechanism behind the cytoxicity of AgNPs is remained contradictory, however, it is speculated that, AgNPs induce cytotoxicity through troazan horse type mechanism, favouring the ionization of NPs inside the cell is the initiator of different toxicity inducing pathway [2]. Thus, stability of NPs might be a fact of toxicity issue. In this study, we found that Com AgNPs are less stable than Brassica AgNPs, suggesting more ionization tendency of Com AgNPs resulting to more toxicity. Therefore, ionized silver easily induce toxicity by initiating toxicity inducing pathway. However, the actual mechanism of toxicity of AgNPs is needed to be further study.

Potentiality of green synthesized AgNPs as antibacterial and antifungal agents is highlighted in the previous reports [54]. Consequently, prior to use AgNPs as an antibacterial agent, it is highly required to evaluate their antibacterial activity. In our study, antibacterial activity of Brassica AgNPs was evaluated by determining their activity against *E. coli* and *Enterobacter* sp. Brassica AgNPs showed potential antibacterial activity against both *E. coli* (Fig. 11) and *Enterobacter* sp. (Fig. 12) at the lowest concentration of 10 ppm. A slight increase of zone of inhibition (ZOI) was observed with the increase of concentration up to 2000 ppm (Fig. 13). It was also reported earlier that AgNPs synthesized from green synthesis routes showed

antibacterial activities against *E. coli* and *Enterobacter* sp. as listed in Table 2. AgNPs synthesized using the extracts of *Azadirachta indica*, Capsicum and Tea leaf showed zones of inhibition against *E. coli* which were recorded as 9 mm [55], 10 mm [56] and 0.5 mm [57], respectively, while AgNPs synthesized using *Brassica rapa* var. *japonica* leaf extract showed higher antibacterial ability as compared with them. However, green synthesized AgNPs using phlomis leaf extract and penicillin showed almost equivalent antibacterial activity against *E. coli* [58, 59]. Moreover, *Azadirachta indica* mediated AgNPs induce 6 mm zone of inhibition against *Enterobacter* sp. [55]. whereas, *Brassica rapa* var. *japonica* leaf extract mediated AgNPs induced 9–15 mm zone of inhibition at different concentrations (Fig. 11). Eventually, in comparison with some other reported green synthesized AgNPs, it is clear that *Brassica rapa* var. *japonica* mediated AgNPs was confirmed to be excellent antibacterial ability.

We found an interesting result of cytotoxicity and antibacterial activity of Brassica AgNPs that in a concentration of 10 ppm, it did not show any cytotoxic effect on PC12 cell while excellent antibacterial activity against gram negative bacteria was found in similar concentration.

Exact mechanism behind antibacterial activity of Brassica AgNPs is still unclear. Therefore, we assume a three steps antibacterial mechanism for our synthesized AgNPs which is also supported by Morones et al. [60]. At first, sufficiently small diameter AgNPs were attached to the cell wall of the bacteria, where positively charged AgNPs were interacted with negatively charged bacterial cell wall and subsequently disrupted their proper function like permeability and respiration. Then AgNPs were entered inside the bacteria caused further damage by the interaction with sulfur and phosphorus containing compounds and destroyed their activity. Thus, AgNPs could interact with DNA which eventually hampered their replication ability resulting of initiation of cell death. Further investigation would be needed to clarify the precise mechanism of antibacterial activity caused by Brassica AgNPs.

Table 1 Effect of AgNPs on cell viability obtained from different sources

Source	Cell line	Conc. (µg/mL)	Cell viability (%)	References
Albizia adianthifolia Leaf extract	A549	10	79	[51]
S. grandiflora leaf extract	MCF-7	5	50	[46]
Humicola sp.	NIH3T3	250	79.17	[53]
Humicola sp.	MDA-MB-231	250	57.82	[53]
Watermelon rind extract	Rat splenocytes	4	67	[15]
Chitosan	HEHEK293	15.07	50	[52]
Commercial AgNPs (< 150 nm)	RAW 264.7	1.6	70	[40]
Commercial AgNPs (13.5 nm)	HeLA	2	20	[47]
Commercial AgNPs (13.5 nm)	U937	2	10	[47]

Fig. 12 Antibacterial activity of Brassica AgNPs to *Enterobacter* sp. in terms of zone of inhibition (ZOI) at a concentration of **a** 10 ppm, **b** 100 ppm **c** 1000 ppm and **d** 2000 ppm. 1, 2, 3 denotes blank, Brassica AgNPs and amphicillin, respectively. Amphicillin and blank represent positive control and negative control as well. Antibacterial activity was repeated for three times for reproducibility

(10 ppm)

(100 ppm)

(1000 ppm)

(2000 ppm)
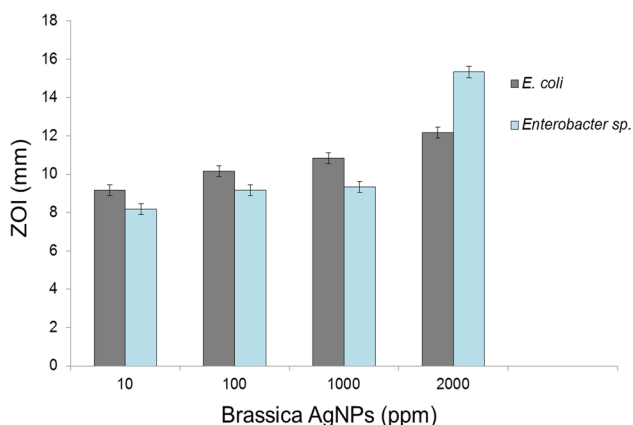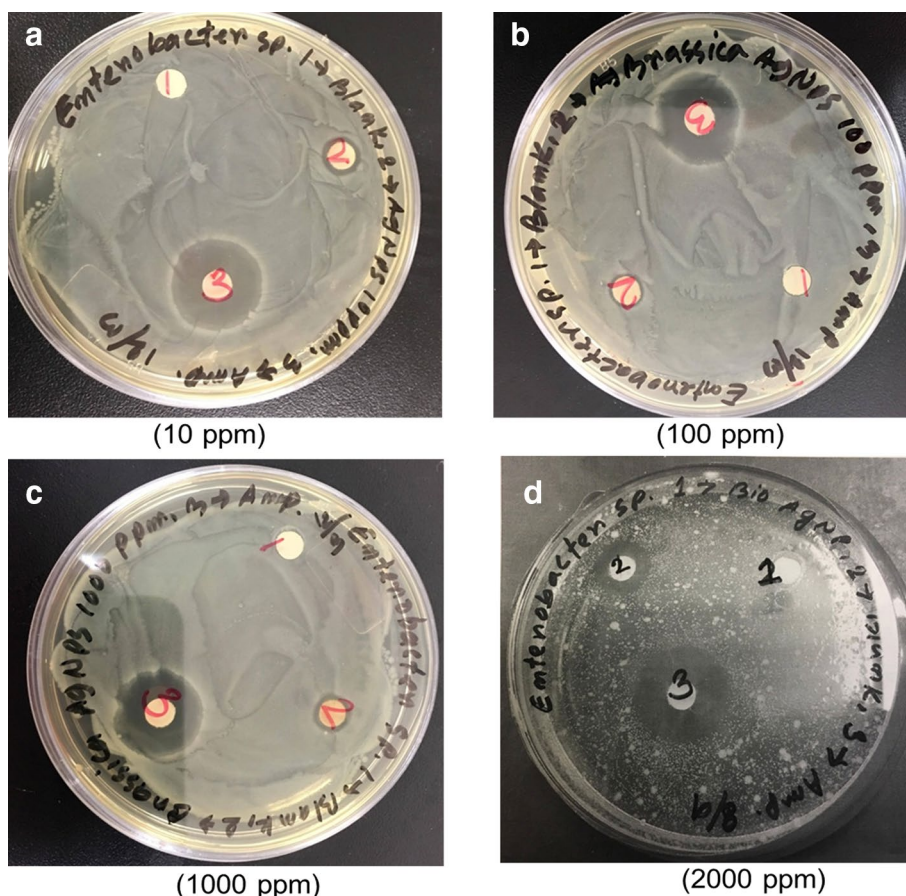
Fig. 13 Antibacterial activity of Brassica AgNPs against *E. coli* and *Enterobacter* sp. in terms of zone of inhibition (ZOI) in different concentrations. Error bars indicate mean ± SD (n = 3)

Table 2 Various green synthesized AgNPs induced zone of inhibition against *E. coli* and *Enterobacter* sp.

Microorganism	Extracted substances	Zone of inhibition (mm)	References
E. coli	*Azadirachta indica*	9	[55]
Enterobacter sp.	*Azadirachta indica*	6	[55]
E. coli	Phlomis leaf	15.1	[58]
E. coli	Tea leaf extract	0.5	[57]
E. coli	Capsicum	10	[56]
E. coli	Penicillin	14	[59]

5 Conclusion

It is the first report of AgNPs showing less toxicity and high antibacterial activity, where *Brassica rapa* var *Japonica* was used as a reducing and capping agent for the synthesis of AgNPs. Crystalline phased Brassica AgNPs showed less toxicity than Com AgNPs on PC12 cells. Moreover, at the same concentration, Brassica AgNPs showed excellent potentiality of antibacterial activity against gram negative bacteria, *E. coli* and *Enterobacter* sp. in comparison with some other reported green synthesised AgNPs. The less cytotoxic activity of Brassica AgNPs might be due to their stability, which was for the presence of capping agent on AgNPs provided by *Brassica rap* var. *japonica*. Therefore, easy and cost effective Brassica AgNPs could be a potential candidate for their safe use in consumer products.

References

1. S. Gajbhiye, S. Sakharwade, J. Cosmet. Dermatol. Sci. Appl. **6**, 48–53 (2016)
2. M. Akter, M.T. Sikder, M.M. Rahman, A.K.M.A. Ullah, K.F.B. Hossain, M. Kurasaki, J. Adv. Res. **9**, 1–16 (2018)
3. J.G. Rouse, J. Yang, J.P. Ryman-Rasmussen, A.R. Barron, N.A. Monteiro-Riviere, Nano Lett. **7**, 155–160 (2007)
4. T. Prow, J.E. Grice, L. Lin, F.N. Rokhaya, M. Butler, W. Becker et al., Adv. Drug. Deliv. Rev. **63**, 470–491 (2011)
5. M. Kreilgaard, Adv. Drug. Deliv. Rev. **54**, 77–98 (2002)
6. S. Kokura, O. Handa, T. Takagi, T. Ishikawa, Y. Naito, T. Yoshikawa, Nanomedicine **6**, 570–574 (2010)
7. Z. Shavandi, T. Ghazanfari, K.N. Moghaddam, Immunopharmacol. Immunotoxicol. **33**, 135–140 (2011)
8. J.H. Sung, J.H. Ji, J.D. Park, J.U. Yoon, D.S. Kim, K.S. Jeon, Toxicol. Sci. **108**, 452–461 (2009)
9. F. Sambale, S. Wagner, F. Stahl, R.R. Khaydarov, T. Scheper, D. Bahnemann, J. Nanomater. (2015). https://doi.org/10.1155/2015/136765
10. J. Mytych, J. Zebrowski, A. Lewinska, M. Wnuk, Mol. Neurobiol. **54**, 1–16 (2016)
11. M.G. Guzmán, J. Dille, S. Godet, Int. J. Chem. Biomol. Eng. **2**, 104–111 (2009)
12. C. Mao, Y. Xiang, X. Liu, Z. Cui, X. Yang, K.W. Yeung, H. Pan, X. Wang, P.K. Chu, S. Wu, ACS Nano **11** 9010–9021 (2017)
13. M. Starowicz, B. Stypula, J. Banas, Electrochem. Commun. **8**, 227–230 (2006)
14. H. Xu, B.W. Zeiger, K.S. Suslick, Chem. Soc. Rev. **42**, 2555–2567 (2013). https://doi.org/10.1039/C2CS35282F
15. P. Velmurugan, S.C. Hong, A. Aravinthan, S.H. Jang, P.I. Yi, Y.C. Song et al., Arab. J. Sci. Eng. **42**, 201–208 (2016)
16. J.L. Gardea-Torresdey, E. Gomez, J.G. Parsons, J.R. Peralta-Videa, J.G. Parsons, H.E. Troiani, J. Langmuir. **19**, 1357–1361 (2003)
17. S.P. Chandran, M. Chaudhary, R. Pasricha, A. Ahmad, M. Sastry, Biotechnol Prog. **22**, 577–583 (2006)
18. J.M. Ashraf, M.A. Ansari, H.M. Khan, A.M.A. Alzohairy, I. Choi, Choi, Sci. Rep. (2016). https://doi.org/10.1038/srep20414
19. A. Narayanamma, IOSR J. Polym. Text. Eng. **3**, 17–25 (2016)
20. S.M. Roopan, G. Madhumitha, A.A. Rahuman, C. Kamaraj, A. Bharathi, T.V. Surendra, Ind. Crops. Prod. **43**, 631–635 (2013)
21. U.B. Jagtap, V.A. Bapat, J. Plant. Biochem. Biotechnol. **22**, 434–440 (2013)
22. G.A. Kahrilas, L.M. Wally, S.J. Fedrick, M. Hiskey, A.L. Prieto, E. Janel, ACS Sustain. Chem. Eng. **2**, 367–376 (2014)
23. F.H. Sahin, T. Aktas, F.E. Acikgoz, T. Akcay, Peer J. Pre Prints (2016) https://doi.org/10.7287/peerj.preprints.1698v1
24. C. Jiang. Y. Yuan, F. Hu, Q. Wang, K. Zhang, Y. Wang et al., Biol. Trace Elem. Res. **158**, 249–258 (2014)
25. S.C. Edberg, E.W. Rice, R.J. Karlin, M.J. Allen, Appl Microbiol. **88**, 1068–1168 (2000)
26. X. Xie, C. Mao, X. Liu, Y. Zhang, Z. Cui, X. Yang, K.W.K. Yeung, H. Pan, P.K. Chu, S. Wu, ACS Appl. Mater. Interfaces **9**, 26417–26428 (2017)
27. Y. Zhang, X. Liu, Z. Li, S. Zhu, X. Yuan, Z. Cui, X. Yang, P.K. Chu, S. Wu, ACS Appl. Mater. Interfaces. https://doi.org/10.1021/acsami.7b17351
28. K. Soo-Hwan, H.S. Lee, D.S. Ryu, S.J. Choi, D.S. Lee, Korean J. Microbiol. Biotechnol. **39**, 77–85 (2011)
29. J.W. Chow, V.L. Yu, D.M. Shlaes, Am. J. Infect. Control. **22**, 195–220 (1994)
30. M.M. Rahman, J. Ukiana, R.U. Lopez, M.T. Sikder, T. Saito, Chem. Biol. Interact. **269**, 41–49 (2017)
31. M.M. Rahman, R.U. Lopez, M.T. Sikder, G. Tan, T. Hosokawa, T. Saito, M. Kurasaki, Chemosphere **196**, 453–466 (2018)
32. M. Saravanan, A.K. Vemu, S.K. Barik, Colloids Surf. B Biointerfaces **88**, 325–331 (2011)
33. Z. Liu, Y. Zhu, X. Liu, K.W.K. Yeung, S. Wu, Colloids Surf. B Biointerfaces **151**, 165–177 (2017)
34. A.K.M.A. Ullah, A.K.M.F. Kibria, M. Akter, M.N.I. Khan, M.A. Maksud, R.A. Jahan, S.H. Firoz, J. Saudi Chem. Soc. **21**, 830–836 (2017)
35. G. Sagar, B. Ashok, Eur. J. Exp. Biol. **2**, 1654–1658 (2012)
36. A.K.M.A. Ullah, A.K.M.F. Kibria, M. Akter, M.N.I. Khan, A.R.M. Tareq, S.H. Firoz, Water Conserv. Sci. Eng. **1**, 249–256 (2017)
37. H.M.B. Alam, R. Das, M. Shajahan, A.K.M.A. Ullah, A.K.M.F. Kibria, Int. J. Hydrog. Energy **43**, 1998–2008 (2018)
38. F. Yang, M. Zhao, B. Zheng, D. Xiao, L. Wu, Y. Guo, J. Matter. Chem. **22**, 25471–25479 (2012)
39. P.H.M. Hoet, I. Bruske-Hohlfeld, O.V. Salata, J. Nanobitechnol. **2**, 1–15 (2004)
40. E.J. Park, J. Yi, Y. Kim, K. Choi, K. Park, Toxicol. In Vitro **24**, 872–878 (2010)
41. C. Krishnaraj, E.G. Jagan, S. Rajasekar, P. Selvakumar, P.T. Kalaichelvan, N. Mohan, Colloids Surf. B Biointerfaces **76**, 50–56 (2010)
42. J. Huang, Q. Li, D. Sun, Y. Lu, Y. Su, X. Yang, Nanotechnology **18**(11), 105104 (2007)
43. K.T. Vadiraj, S.L. belagali, J. Mater. Sci. **27**, 2885–2889 (2016)
44. G. Sathishkumar, C. Gobinath., K. Karpagam, V. Hemamalini, K. Premkumar, S. Sivaramakrishnan, Colloids Surf. B Biointerfaces **95**, 235–240 (2012)
45. Y.H. Hsueh, K.S. Lin, W.J. Ke, C.T. Hsieh, C.L. Chiang, PLoS ONE (2015) https://doi.org/10.1371/journal.pone.0144306
46. M. Jayaraj, G. Sathishkumar, G. Sivanandhan, A. Mubarak, M. Rajesh, R. Aurun, Colloids Surf. B Biointerfaces **106**, 86–92 (2013)
47. S.I. Kaba, E.M. Egorova, Nanotechnol. Sci. Appl. **8**, 19–29 (2015)
48. S. Kim, J.E. Choi, J. Choi, K.H. Chung, K. Park, Y. Jongheop, et al. Toxicol. In Vitro **23**, 1076–1084 (2009)
49. S. Arora, J. Jain, J.M. Rajwade, K.M. Paknikar, Toxicol. Lett. **179**, 93–100 (2008)
50. S.M. Hussain, K.L. Hess, J.M. Gearhart, K.T. Geiss, J.J. Schlager, Toxicol. In Vitro **19**, 975–983 (2005)
51. R.M. Gengan, K. Anand, A. Phulukdaree, A. Chuturgoon, Colloids Surf. B Biointerfaces **105**, 87–91 (2013)
52. M.P. Noghabi, M.R. Parizadeh, M.G. Mobarhan, D. Taherzadeh, H.A.H.M. Darroudi, J. Mol. Struct. **1146**, 499–503 (2017)
53. S.S. Saraswati, G.C. Kundu, A. Ahmad, Spectrochim. Acta A Mol. Biomol. Spectrosc. **114**, 144–147 (2013)
54. P. Velmurugan., M. Iydroose., M.H. Mohideen. T.S. Mohan, M. Cho, B.T. Oh, Bioprocess. Biosyst. Eng. **37**, 1527–1534 (2014)
55. K. Renugadevi, R.V. Aswani, Int. J. Nanomater. Biostruct. **2**, 5–10 (2012)
56. A.A. Abdullah, Z.U. Hamid, J. Biol. Agric. Healthc. **3**, 67–71 (2013)
57. Q. Sun, X. Cai, J. Li, M. Zheng, Z. Chen, C.P. Yu, Colloids Surf. A Physicochem. Eng. Asp. **444**, 226–231 (2014)
58. A.R. Allafchian, S.Z. Mirahmadi-Zare, S.A.H. Jalali, S.S. Hashemi, M.R. Vahabi, J. Nanostruct. Chem. **6**, 129–135 (2016)
59. I. Maliszewska., Z. Sadowski, J. Phys. **2009**, 146 (2009). https://doi.org/10.1088/1742-6596/146/1/012024
60. J.R. Morones, A.C. Elechifuerra, K. Holt, J.B. Kouri, J.T. Ramirez, M.J. Yacaman, Nanotechnology **16**, 2346–2353 (2005)